

Educational Software/Structural Monitoring

Finite element implementation for computer-aided instruction of structural mechanics
*Jae Young LEE**, *Sung-Youll AHN (Chonbuk National University)*

MASTAN2, educational analysis software for the 21st century
Ronald D. ZIEMIAN (Bucknell University), William McGuire (Cornell University)*

Spot monitoring and time-dependent analysis of high-rise building construction process
Shenwei ZHANG (Shandong University), Qilin ZHANG, Xin LOU (Tongji University)*

A model-based framework for real-time structural monitoring in uncertain environments
Phaedon-Stelios KOUTSOURELAKIS (Cornell University)

Prediction of maximum deflection of double layer grid space structure using neural networks
Reza KAMYAB MOGHADAS (Iranian Academic Center for Education, Culture and Research), Kok Keong CHOONG, Sabarudin MOHD (Universiti Sains Malaysia)*

For multiple-author papers:

Contact author designated by *

Presenting author designated by underscore

Finite element implementation for computer-aided instruction of structural mechanics

Jae Young LEE*, Sung-Youll AHN

*Dept. of Regional Construction Engineering, Chonbuk National University
Chonju 561-756, Korea
jylee@chonbuk.ac.kr

Abstract

A new approach of computer-aided instruction is proposed for education of structural mechanics and other related subjects. The instructional tools are operated with the user-created modeling data and their ensuing analysis results on the basis of finite element technology. They are devised to promote the understanding, and to stimulate the interest in the subjects by substantiating the conceptual principles and visually exhibiting the complex computational processes with the aid of interactive computer graphics.

1. Introduction

Many commercial finite element analysis programs are available for solving various problems in the fields of engineering and physical science. They are widely adopted also as instructional software by academic courses in many disciplines. However, their role for instruction is limited either to training of their own usage or to their application in practice, but not extended to education of the academic substance itself in the subjects of application. VisualFEA, a finite element analysis program, has the uniqueness in its native instructional capability to assist teaching or learning the fundamental concepts, principles and methods in structural mechanics and other related subjects. The user-friendliness and ease-of-use are the basic requirements of the educational functions (Abel [1], Hilheim [2]). The contents of the tools should possess the ingredients to stimulate the interest in the study of the subjects. VisualFEA pursues the standard with the following features:

- Graphical manipulation and visualization
- Operation with user created analysis model
- Generalized application of finite element processing
- Results adapted to conventional approaches

We expect that the use of these instructional tools will produce the following educational effects,

- Enhancement of the understanding on conceptual subjects through visualization
- Learning by experience through interactive simulation
- Familiarization with computing methods by observing the process and the result with realistic data
- Trial-and-error learning through repeated real-time operations
- Effect of self training and practicing

The instructional functions presently available in VisualFEA can be categorized into two parts, items for education of structural mechanics and others for finite element method (Lee [3],[4]).

2. Instructional aids for structural mechanics

Interactive computer operations and graphical visualizations are extensively employed to aid the instruction of conceptual principles, computing formula and analysis methods in the classical structural mechanics.

2.1 Structural response to applied conditions

Interactive manipulation of input data such as material properties, applied loads and support state, and the consequent real-time analysis and rendering will help the users to build a good sense of presumption about the structural behavior under various conditions. Graphical animation is employed to deliver the dynamic behavior.

2.2 Mathematical relationship of shear force, bending moment and deflection

As shown in Figure 1, the diagrams of shear force, bending moment and deflection of beams are drawn in parallel so that their inter-relationships are indicated conspicuously. The diagram area, slope, curvature, zero crossing points, and mini-max points are dynamically highlighted in response to user's operation. Such graphical visualization will help reasoning and understanding the mathematical relationships between the diagram items.

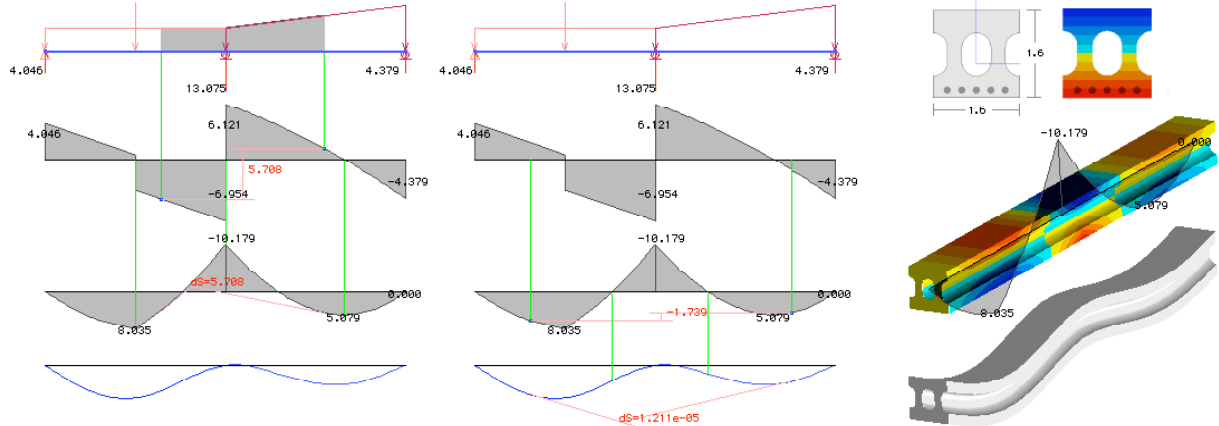


Figure 1: Inter-relationship of stresses, forces and deflection

2.3 Stresses on the frame member section

The cross sections of frame members can be defined either in freeform or in preset geometric shape. The sectional constants, stresses, internal forces and moments are instantly computed and displayed as soon as the necessary data are supplied or modified. The stress images suggestive of the computational aspects are rendered along the span and over the cross section, and updated instantly following any data change so as to give the insight on the structural behavior. The user may add sectional reinforcements and examine the resulting effects.

2.4 Influence line

The influence line is a conventional but still useful concept in structural mechanics. VisualFEA constructs the influence lines of a statically determinate or indeterminate frame by combining a series of finite element solutions with multiple loading cases. This function helps the user to emulate the drawing of influence lines for various conditions, and thus to understand the variation of the internal forces due to the changing load position.

2.5 Moving load

The minimum and maximum stress resultant envelopes of interconnected moving loads are useful as practical information for structural designs. In VisualFEA, this function is implemented for educational use as well as for practical application. While the position of the loads is being moved interactively, the consequently changing diagrams of bending moment or shear force are overlaid with the envelope diagrams. This interactive and dynamic display provides various information explanatory of moving load concept and its significance.

2.6 Mohr circle

VisualFEA draws the Mohr circle for the solution data sampled at the mouse-clicked point of an actual finite element model, instead of arbitrarily assumed data. Such an approach is more plausible in getting the sense of the real and also in understanding the context and the usage of Mohr circle. While the user is setting or changing the direction of the stress plane, the Mohr circle is refreshed on the σ_n - τ plane. At the same time, an inclined rectangle is drawn with stress components on the sampling point as shown in Figure 2. The principal stresses, the maximum shear stresses and their directions are instantly drawn on the σ_n - τ plane and on the stress point in response to the user actions. In case of a 3-D solid model, the Mohr circle is represented by threesome circles on σ_n - τ plane, and the direction of stress planes are rendered by a cube at the sampling point.

2.7 Elasto-plastic yielding

The representation of failure envelope on the σ_n - τ plane or the mean-deviatoric stress plane will be very effective in delivering the concept of the elasto-plastic failure theories. As exemplified in Figure 2, the Mohr-

Coulomb theory of plastic yielding due to load increment is clearly revealed by a series of Mohr circles bounded by the line of failure envelope.

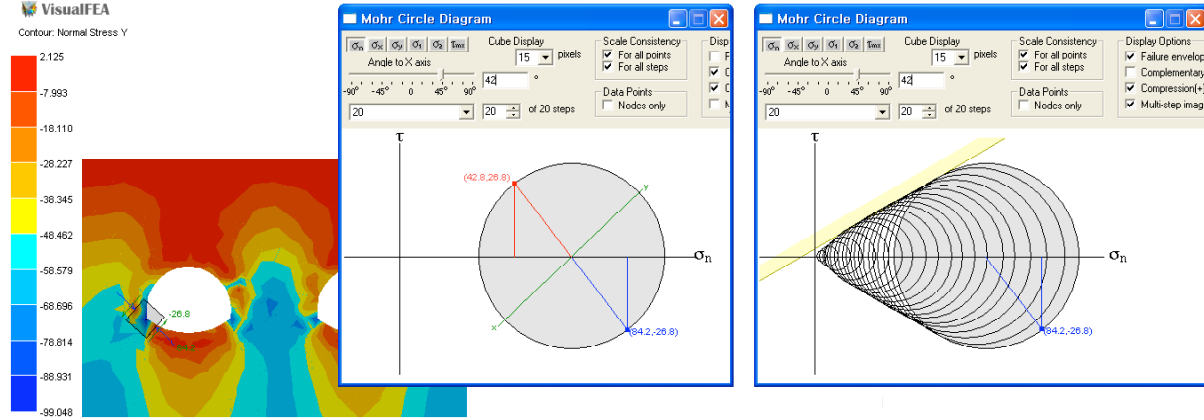


Figure 2: Mohr circle and failure envelope

2.8 Stress path on the yield surface

VisualFEA has the function of visualizing the yield surface and the stress path in the principal stress space defined by σ_1 - σ_2 - σ_3 axes. The progress of yielding is expressed by the graphical image of the stress path creeping over the yield surface. Such visualization is the most effective method of describing the concept of the yielding process that may look ambiguous otherwise to the students. The axes of the space may represent other parameters. For example, the yielding of CamClay models may be visualized using the stable state boundary surface in the space of mean stress (σ_m), deviatoric stress (σ_d) and void ratio (e) as shown in Figure 3.

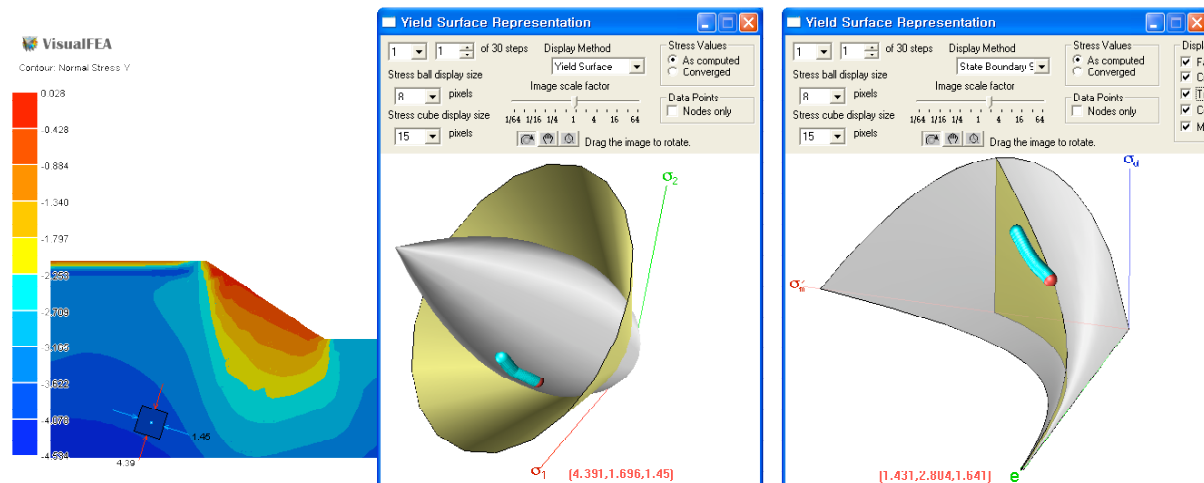


Figure 3: Stress path on the yield surface and the stable state boundary surface of a CamClay model

3. Computer-based education of finite element method

Numerical exercise and computer programming are the best ways of understanding and mastering the concepts and procedures of the finite element method, but demand considerably rigorous efforts. The difficulty may be relieved by the function of simulating the finite element procedures as provided in VisualFEA.

3.1 Stiffness matrix assembly and solution process

VisualFEA has the function of simulating and visualizing the stiffness computation, assembly and solution processes. Various contents of computation at the element stiffness level are displayed either numerically or

symbolically in tree-view expansion style. Assembly of the global system equations can be simulated by drag-and-drop or step-by-step operations. Users may get indirect experience of assembling and solving the system equations for finite element analysis through such interactive operations as shown in Figure 4.

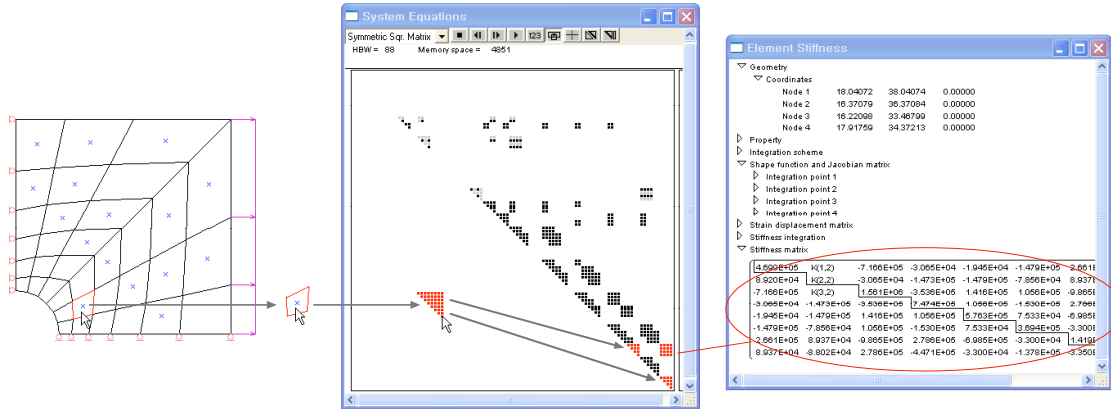


Figure 4: Computation and assembly of stiffness matrix

3.2 Shape function and interpolation

The shape functions and their derivatives can be visualized as 2-D or 3-D graphic images, which help understanding the nature and the variation of shape functions. The order of continuity such as C^0 , C^1 and C^2 , within an element and across adjacent element boundaries can be demonstrated easily by this function.

3.3 Eigenmodes

Eigenvalues and corresponding eigenvectors are extracted from the stiffness equations of a static or a dynamic analysis, and visualized as displacements or vibrations. They are arranged so as to give insight into the system characteristics such as rigid body modes, spurious zero energy modes, dynamic modes, etc. The physical interpretation of the eigenmodes can also be reviewed in conjunction with element types and integration orders.

3.4 Stress smoothing

The stress recovery and smoothing procedure can be experimented and inspected by interactive simulation. The computational aspects and characteristics are recapitulated and understood easily using this educational function. Different methods of recovery and smoothing can be compared with each other.

3.5 Process of adaptive analysis

VisualFEA has the capability of reproducing the multi-step mesh refinement, error evaluation, and adaptation process for step-by-step examination under user control. The function is devised to help understanding the principles and the methods of adaptive solution procedure.

4. Conclusion

Computer-aided instructional tools for structural mechanics and other related subjects were implemented on the basis of finite element technology. They have been experimented in actual education, and proved to be very effective as teaching and learning devices. New items of instructional functions are continuously being added to VisualFEA so that most of the topics in this field of study are covered eventually by the computer-aided instruction. This work will proceed forward to set a new paradigm of education in engineering.

References

- [1] Abel JF, Interactive graphics as a stimulus to creative play in engineering education, *Proceedings of the International Conference on Computer Aided Training in Science and Technology*, Barcelona, 1990;66-72.
- [2] Hilheim, WD, Computer-based simulations in education and training, Educational Technology Pub., 1992.
- [3] Lee JY, Development of a computer-based training system for finite element method, *Journal of the Computational Structural Engineering Institute of Korea*, 1999; **12-4**:607-618.
- [4] Lee JY, VisualFEA/CBT, computer-based training of finite element method, John Wiley and Son's, 2002.

MASTAN2, educational analysis software for the 21st century

Ronald ZIEMIAN*, William MCGUIRE

* Dept. of Civil Engineering, Bucknell University
Lewisburg, PA 17837 USA
ziemian@bucknell.edu

Abstract

Fueled by major advances in computer graphics and hardware, commercial structural analysis software continues to become easier to use while at the same time providing an increased number of available linear and nonlinear analysis features. Unfortunately, with this increased user-friendliness and sophistication, there comes a potentially dangerous consequence of encouraging their use as a “black box”. In an effort to discourage this practice in academia, and instead facilitate the teaching of the underlying principles and assumptions on which this software is based, the authors have developed the educational structural analysis program MASTAN2. This paper provides an overview of the MASTAN2 software and further shows how such software can be used as a tool in undergraduate and graduate level courses.

1. Introduction

Over the past ten years, the authors have informally tracked several curricula in the U.S. and have noted a disturbing trend within structural analysis courses. Originally, such courses had a significant component, or in many cases an entire course dedicated to teaching the direct stiffness method, a finite element approach to truss and frame analysis. These courses not only included theoretical derivations and hand calculations, but also a significant component of computer programming. Such programs were often written in FORTRAN and provided the student with the opportunity to fully comprehend the logic employed and the limitations within equivalent commercial analysis software.

The above study was in some cases part of an advanced structural analysis course in a four-year undergraduate curriculum, but more often contained within a graduate course on matrix structural analysis. In either case, the student needed to be proficient in both the basics of structural analysis and just as importantly, a programming language.

In more recent years, the authors have observed a significant reduction in emphasis being placed on fully learning the direct stiffness method. The following reasons are suggested as possible contributors:

- There has been a reduction in the number of structural analysis courses offered within undergraduate curricula. Hence, the direct stiffness method is often only being taught at the tail end of an introductory analysis course. In many cases, the topic and especially the programming requirements are considered too advanced for an undergraduate curriculum.
- Similarly, it appears that graduate school curricula in structural engineering are also cutting back on the number of analysis courses being taught. Instead of offering a full course in the matrix structural analysis of frames and trusses, this topic is being covered briefly at the beginning of a comprehensive finite element course that also covers two- and three-dimensional continuum elements, including planar, axisymmetric, brick, and shell elements. Such courses often include a significant component on nonlinear analysis. In any case, the reduced coverage of frame and truss elements is considered more or less a review, which is justified by the perhaps erroneous assumption that students have fully learned the direct stiffness method as part of their undergraduate education.

- Industry is placing more emphasis on hiring students who are proficient in the use of commercially available structural analysis software packages. Although these packages often provide excellent graphical user interfaces that make them easy to use, the number of available pre- and postprocessing features make such software quite time consuming to introduce and employ within structural analysis courses.
- Most undergraduate civil engineering curricula are no longer requiring full courses in a structured programming language such as FORTRAN, C, or C++. Instead, programming knowledge is either being removed from the curriculum or being taught as a small part of an engineering computation course. In most cases, these courses are based on MATLAB®, a premier software package for numeric computing and data analysis distributed by the MathWorks, Inc.

Confronted with this current situation, but also realizing that a vast majority of civil engineering systems analyzed by future practicing structural engineers will continue to be two- and three-dimensional trusses and frames, the authors have developed the educational structural analysis program MASTAN2. The program, which is described in the remainder of this paper, is currently being used at over 100 universities throughout the U.S. and several universities in Europe, South America, Australia, and Asia. The program comes in two versions and is available at no cost at www.mastan2.com. The stand alone version runs on any PC platform, and for those interested in programming their own user-defined code or additional features, a MATLAB based version is also available.

2. Overview of MASTAN2

In many ways, MASTAN2 is similar to today's commercially available software in functionality. However, the number of pre- and postprocessing options has been purposely limited in order to minimize the amount of time needed for a user to become proficient at its use. In this way, students find a logical transition in eventually moving from the MASTAN2 graphical user interface to commercial software. Just as important, faculty can introduce the MASTAN2 software within a single lecture hour. The program's linear and especially its nonlinear analysis routines are comprehensive and reflect future trends in the structural engineering design profession. All of the analysis routines are based on the theoretical and numerical formulations presented in an associated textbook written by the authors [1]. In this regard, the use of this software is strongly encouraged as a tool for demonstration, reviewing examples, solving problems, and perhaps performing analysis and design studies. Since MASTAN2 has been written in modular format and is based on MATLAB, students are also provided the opportunity to develop and implement additional or alternative analysis routines directly within the program.

Preprocessing options within MASTAN2 include definition of structural geometry, support conditions, applied loads, and element properties. The analysis routines provide the user the opportunity to perform first- or second-order elastic or inelastic analyses of two- or three-dimensional frames and trusses subjected to static loads. Postprocessing capabilities include the interpretation of structural behavior through deformation and force diagrams, printed output, and facilities for plotting response curves.

3. Analysis Capabilities

The most common levels of structural frame analysis are represented in Figure 1 by schematic response curves for a statically loaded frame. The degree to which they can model true behavior differs, but each can provide information of value to the engineer.

By definition, first-order (linear) elastic analysis excludes nonlinearity; the equations of equilibrium are formulated on the undeformed structure and the material is assumed elastic. In second-order analysis, the effects of finite deformations and displacements are accounted for in formulating the equations of equilibrium. In an inelastic analysis, material nonlinear behavior is taken into account. In addition to these incremental procedures, a critical load analysis determines the load at which both the original and an alternative loading path become mathematically valid and it can be shown that the alternative path will be the one taken from that point.

In the curves shown, various possibilities for changing rates of nonlinear response are indicated. Of particular interest is increasing nonlinearity culminating in a decrease in resistance at an elastic or inelastic stability limit. This is probably the most common mode of failure in civil engineering structures.

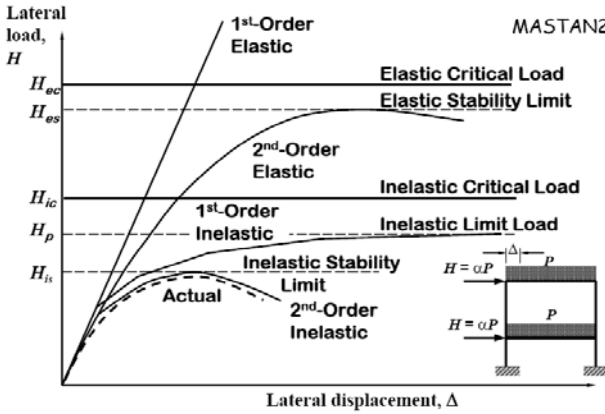


Figure 1: Levels of analysis offered in MASTAN2

The MASTAN2 software was developed to illustrate the design potential of these contemporary computer methods. A bisymmetrical 14 degree-of-freedom element is employed within the program. The basic underlying matrix equations are:

$$\text{1st-order elastic: } [K_e]\{\Delta\}=\{P\} \quad (1)$$

$$\text{2nd-order elastic: } [K_e+K_g]\{d\Delta\}=\{dP\} \quad (2)$$

$$\text{1st-order inelastic: } [K_e+K_m]\{d\Delta\}=\{dP\} \quad (3)$$

$$\text{2nd-order inelastic: } [K_e+K_g+K_m]\{d\Delta\}=\{dP\} \quad (4)$$

$$\text{Critical loads: } [K_e+\lambda K_g]\{d\Delta\}=\{0\} \quad (5)$$

in which K_e is the elastic stiffness matrix and K_g a corresponding geometric stiffness matrix. K_m is a plastic reduction matrix that represents the change in stiffness that results from the formation of one or more plastic hinges. Material nonlinear behavior is controlled by the combination of a yield surface and a tangent modulus provision. K'_g is the geometric stiffness matrix computed for a reference load $\{P_{ref}\}$, and λ is the critical load factor with respect to this reference load. By modifying the material constants in K_e , (5) can be used to calculate inelastic critical loads in accordance with a concept such as the tangent modulus theory.

3. Simple Example

A fairly flexible steel frame is used to illustrate the MASTAN2 analysis capabilities (Figure 2). Through the use of this software, students can see first hand the different ways in which geometric and material nonlinear behavior, alone or in combination, can contribute to a structural instability. In addition to providing students with fairly advanced analysis capabilities, such an example can show how various levels of analyses can enhance understanding of the behavior of a particular structural system and in turn, aid in the efficient proportioning of its components.

4. Programming Opportunities

Since MASTAN2 has been written in a modular format that is based on MATLAB, students are also provided the opportunity to develop and implement additional or alternative analysis routines. The interface between MASTAN2 and the student's code is provided through the use of a common MATLAB file. For example, the function contained in the MASTAN2 text file `ud_3d2el.m` is called when a user selects the corresponding menu options and then applies a three-dimensional second-order elastic analysis. Once the student makes this analysis option functional by expanding the code contained in this file, an analysis will be performed. Of course, the code the student provides may also call other student prepared functions, providing the opportunity to write code in a modular style. The first line in a MASTAN2 interface file such as `ud_3d2el.m` takes on the form

```
function [output] = ud_3d2el(input)
```

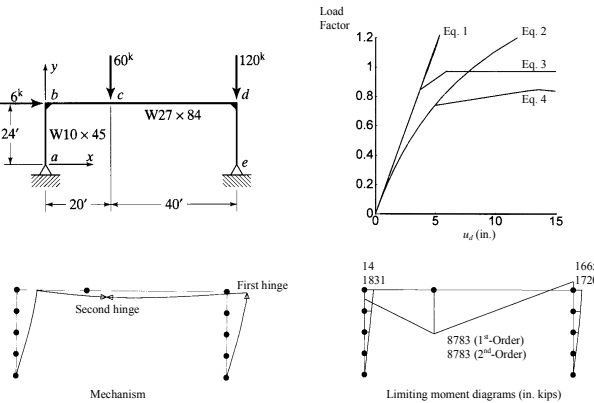


Figure 2: Steel frame example

where the input is a series of arrays defined by MASTAN2 that contain all geometric, material, support, and loading information. The output arrays, again with format defined by MASTAN2, would contain the displacements, element forces, and reactions calculated by the student's user defined code.

There are a total of twelve well-commented interface files which permit a student to prepare user defined code that emulate all of the MASTAN2 linear and nonlinear analysis features previously described for both two- and three-dimensional structural systems.

Although some universities continue to have their students write all parts of the routines needed to perform a certain level of analysis, several schools make use of available MATLAB structural analysis toolboxes. Using what is often described as a building block approach, students still have the opportunity to prepare an analysis package but instead of detailed programming assignments they use a series of prepared modular routines, e.g. a predefined function that generates an element stiffness matrix for a planar frame element or a routine that assembles the global stiffness matrix from the element stiffness matrices. An excellent and popular example of this type of structural analysis toolbox is CALFEM (abbreviation for "Computer Aided Learning of the Finite Element Method".) which is developed at the Division of Structural Mechanics, Lund University [2]. By combining the pre- and post-processing capabilities of MASTAN2 with the analysis routines provided in a toolbox such as CALFEM, students (especially at the undergraduate level) can be provided the opportunity to prepare analysis code within a limited course schedule.

5. Summary

Using the authors' perspective on the current state of teaching modern methods of structural analysis at undergraduate and graduate school programs, a case is made for the development of the educational structural analysis software MASTAN2. An overview of the pre- and post-processing options as well as the linear and nonlinear analysis capabilities contained within MASTAN2 is then presented. An example showing typical results is provided. The paper concludes with a section that shows how students with access to MATLAB can prepare analysis code that can interface with MASTAN2. This code may be fully prepared by the student or, depending on course requirements, the student may be able to take advantage of a MATLAB structural analysis toolbox such as CALFEM. In all cases, the MASTAN2 software is intended to encourage faculty to continue to teach students how computer analysis programs obtain solutions, as opposed to teaching students how to simply become proficient in using specific commercial software products.

References

- [1] McGuire, W, Gallagher, RH, Ziemian, RD. Matrix Structural Analysis (2nd edn). John Wiley and Sons, Inc., 2000.
- [2] Austrell, P, Dahlblom, O, Lindemann, J, Olsson, A, Olsson, K, Persson, K, et al., CALFEM, A Finite Element Toolbox, Division of Structural Mechanics, Lund University, 2004.

Spot monitoring and time-dependent analysis of high-rise building construction process

Shenwei ZHANG*, Qilin ZHANG, Xin LOU

*School of Civil Engineering Shandong University
73 Jingshi Road, Jinan, 250061, Shandong Province, China
Sduzsw@sdu.edu.cn

Abstract

The expanding of construction scale and the complexity of structure system bring out the complexity and safety problem in the construction process, which can result in that the construction procedures have great effect on the final state of structures. Based on the time-dependent model of reinforced concrete in CEB-FIP MD90, the numerical simulation of the construction process of CFST structures are provided in this paper. The spot timely monitoring test with vibrating strain gauge was conducted during the construction of Tongji multifunctional building, the comparison of the test results and the numerical simulation results demonstrated that the method in this paper could precisely simulate the time-dependent force and deformation of structures during the construction process, and the numerical simulation results showed that the deformation of the structure resulted from the shrinkage and creep of concrete during construction can not be ignored in the design.

1. Introduction

The expanding of construction scale and the complexity of structure system bring out the complexity and safety problem in the construction process, which can result in that the construction procedures have great effect on the final state of structures. And the difference of the construction stage would yield to the age variance of the structural members, which result in the difference of structural members in elastic modulus and material property. Especially the effect of creep, shrinkage, strength and other factors lead to the complexity of construction analysis for composite structures, because the above factors changing continuously not only in the construction process but also in the service period will cause the redistribution of inner force in the structures.

In order to estimate the force during the construction process, it was necessary to conduct the construction process analysis considering to the time dependent model of material. In the long term load, the creep effect was one of the basic properties of concrete; and creep of concrete would result in the change of deformation and force redistribution, which would affect the long term service of structures. The domestic and international researchers had carried out a lot of research on the mechanics of creep and proposed many models of creep [1-3]. The creep effect in concrete bridge, concrete filled steel tube and mass concrete had been extensively studied [4-6], and for the high rising buildings and super high rising buildings with symmetry array of structure and uniform load distribution in the structures , the researchers mainly focused on analyze the vertical deformation difference between the tube structure and frame structure[6-8]. While for the structure with unsymmetrical array and non-uniform load distribution, the non-uniform deformation resulted from creep of concrete in long term load would affect the regular service and even the safety of the structures.

2. Time dependent nonlinear theory of concrete filled steel tube

The time dependent nonlinearity related to the high-rising building construction mainly referred to the time dependent nonlinear deformation and inner force resulted from shrinkage and creep of concrete composite structures, and in the construction process simulation of this kind of structures, the time dependent effect of strength and elastic modulus in the whole construction process should be considered. The time dependent effect mainly referred to the shrinkage, creep, strength and elastic modulus varied with the increasing of time. And the relationship between the time dependent effect and load was not linearity, so the time dependent nonlinearity was involved in this paper. As a result, the time dependent model should be firstly selected to ensure the

accuracy of the construction process analysis. In this paper, the time dependent model in CEB-FIP MD90 [9] was used in the analysis of high rising buildings.

2.1 Time dependent model of concrete strength and elastic module

The time dependent model of concrete strength in CEB-FIP MD90 was [9]

$$f_{cm}(t) = \eta(t)f_{cm}, \quad E_c(t) = E_{c,28}\sqrt{\eta(t)}, \quad \eta(t) = \exp[s(1 - \sqrt{28/t})] \quad (1)$$

In which, $f_{cm}(t)$ was the average compress strength, f_{cm} was the average compress strength for the 28th days, $\eta(t)$ was the coefficient relation to the age of concrete, s was a constant corresponding to the kind of cement. $E_{c,28}$ is the elastic modulus of concrete for age 28 days. And the elastic modulus for age 28 days regressed from the test was

$$E_{c,28} = \frac{10^5}{2.2 + 31.5/f_{cu}} \quad (2)$$

The above elastic modulus formula was only suitable for the common concrete consisting with medium sand and igneous rock.

2.3 Shrinkage and creep model of concrete

In the real structures, the elastic strain, creep strain, shrinkage strain and temperature strain mixed together and could not be separated easily. In the numerical analysis, the elastic strain and temperature strain were calculated independently, while the creep strain and shrinkage strain were considered together. Many types of model of time dependent model of creep strain and shrinkage strain for concrete in the reference, this paper only provided the model in CEB-FIP MD90 [9].

2.3.1 Shrinkage strain

The shrinkage strain of concrete was usually described as the product of ultimate shrinkage strain value and the time function of shrinkage strain, i.e.,

$$\varepsilon_s(t, \tau) = \varepsilon_s(\infty, 0)\varphi_s(t - \tau) \quad (3)$$

2.3.2 Creep strain

The creep strain of concrete was usually described with the time function of creep coefficient. $\varepsilon_c(t, \tau)$ was the creep strain from time τ to time t on the stress $\sigma(\tau)$ on time τ , that is:

$$\varepsilon_c(t, \tau) = \frac{\sigma(\tau)}{E_{c,28}}\varphi_c(\infty, 0)\varphi_c(t - \tau) \quad (4)$$

The above time dependent models of concrete were the basis of this high-rise building construction analysis.

3. Engineering example

3.1 Introduction

Tongji multi-functional building with 21stories is located in the northeast of Tongji University campus; it has floor area of 46240m² and 100m in height. The novelty and unique architecture form, spiral rising plane layout and even the installation of the equipment interlayer bring great challenge for the design of the structures. In order to improve the earthquake-resistance of the structure, 56 nonlinear rate-dependent viscous dampers were installed in the structure, and the earthquake model test proved that this structure had excellent earthquake-resistance performance. This kind of structures shown in Fig. 1 was firstly used in china. The frame structure of this building with concrete filled steel tube columns and steel I beams was unsymmetrical in structural layout and complex in stress, for which the stresses in the structural members were more complex during the construction. So, in order to guarantee the safety of the structure during the construction, the spot monitoring

test was conducted and got the stress of the column during construction, and the test results were compared with the numerical analysis results. The vibrating strain gauge was employed to monitor the stress in the column during construction, which was shown in Fig. 2.



Figure 1: Tongji multi-functional building



Figure 2: monitoring system

3.2 Numerical model

The beam element was used to simulate the members of the structures in the finite element model of the structure. And the steel was Q345 and the design strength of concrete was C40. The time dependent models of concrete were those in CEB-FIP MD90 described above.

3.3 Numerical simulation of construction process considering the time-dependent effect of concrete

All the columns in this structure were concrete filled steel tube columns, and for the concrete was a kind of time dependent material, i.e. the strength and elastic module were increasing along with time, the shrinkage and creep of concrete during the process of construction could result in the inner force, which could not be neglected in the design of this kind of structures. In this paper, on the basis of time dependent model in CEB-FIP MD90, numerical simulation of construction process for concrete filled steel tube composite structures was conducted and the numerical simulation results was compared with the spot monitoring test results.

Considering the construction process of the structure and according to the time dependent analysis of concrete filled steel tube composite structures, the vertical deformation curve of the columns were shown in Fig.3 which included the shrinkage deformation, creep deformation, elastic deformation and total deformation . Meanwhile, the deformation of the traditional analysis taking no account of the construction process of the structure was shown in Fig. 3

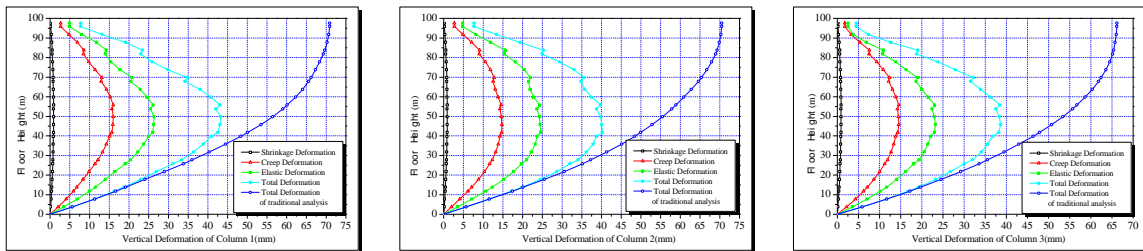


Figure 3: Deformation curve of columns

From the deformation curve shown in Fig. 3, conclusion could be made out that the shrinkage deformation was very small and the creep deformation was very large, which was about 50% of the elastic deformation and 1/3 of the total deformation. As a result, the construction process analysis considering the time dependent effect of concrete should be taken into account for the design of concrete filled steel tube composite structures, and the deformation resulted from the shrinkage and creep especially the creep deformation should not be neglected. The vertical deformations calculated from the traditional design method and the construction process analysis were distinctive. The maximum vertical deformation from the traditional design method located in the top of the structure and the maximum vertical deformation from the construction process analysis was in the middle of the

structure. The maximum value of traditional design method was about 50% higher than that of the construction process analysis.

Considering the construction process and the time dependent effect of concrete, the stress curve of the columns were shown in Fig.4 which included the stress resulted from shrinkage, creep and elastic effect. Meanwhile, the total stress and the spot monitoring stress were also shown in Fig. 4.

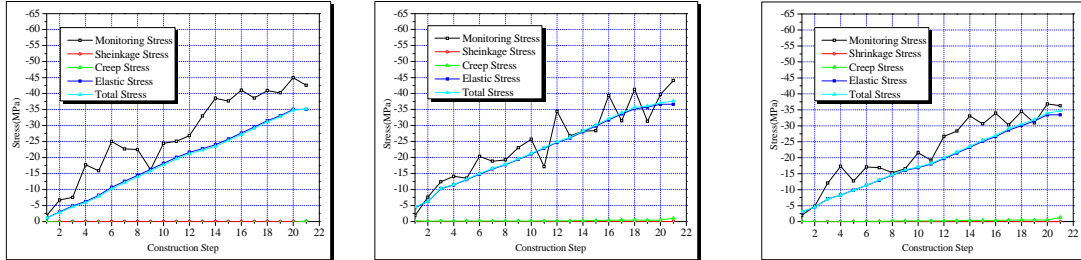


Figure 4: Stress curve of columns

The stress curve shown in Fig.4 demonstrated that the shrinkage and creep stress was very small, which was about 5% of the elastic stress. As a result, the creep and shrinkage deformation had great proportion in the total deformation, but the creep and shrinkage stress was very small compared with the elastic stress.

The comparison of test results and numerical results showed that the regularity of the results was similar, but the values were difference. The causes that lead to the difference were concluded as: load error, effect of measure equipment, model error, environmental influence and so on. For these reasons, the difference between the test results and numerical results was unavoidable.

4. Conclusions

Based on the time dependent model of concrete in CEB-FIP MD90, spot monitoring test and numerical analysis was conducted for a high rising building, and the comparison between test results and numerical results showed that the regularity of the results was similar, but the values had some difference for some reasons. If the effect of the objective reason was decreased, the numerical analysis could simulate the construction process accurately, which could provide reference for the construction.

References

- [1] Ravi Kumar Sharma, Savita Maru, Nagpal A K, "Simplified Procedure for Creep and Shrinkage Effects in Reinforced Concrete Frames", *Journal of Structural Engineering* 2004; 10: 1545-1550.
- [2] ZHOU LV, XU YONGCHUN, Shrinkage and creep, Chinese Railway Publishing Co., Beijing, 1994.
- [3] Gao Zhengguo, Huang Dahai, Zhao Guofan, "A Method for Creep Stress Analysis of Concrete Structures", *China Civil Engineering Journal* 2001; 4: 10-14.
- [4] Lionel Bellevue P E, Paul J, Towell P E. Parsons Brinckerhoff Quade, "Creep and Shrinkage Effects in Segmental Bridges", Advanced Technology in Structural Engineering, Structures Congress 2000, ASCE:2004.
- [5] Huangmin, Dengshujuan, "Creep and Shrinkage Analysis for Buildings", *Journal of Southwest University of Science and Technology* 2004; 3: 49-51.
- [6] Deng Zhiheng, Qin Rong, "Influence of Shrinkage and Creep on High-rising Building in Construction Proceeding", *Journal of Harbin University of C.E. & Architecture* 2002;5: 28-31.
- [7] Luo Xiaohua, "Calculation of Vertical Deformation for Super High Rising Building", *Structural Engineers* 2004; 6: 30-33.
- [8] Fu Xueyi , Sun Can and Wu Bing, "Analysis of Creep Effect on Tall and Super Tall R.C. Buildings", *Journal of Shenzhen University Science and Engineering* 2006;4:283-289.
- [9] CEB-FIP MD90 Model Code 1990, Design Code(s), 1991.

A model-based framework for real-time structural monitoring in uncertain environments

Phaedon-Stelios KOUTSOURELAKIS*

* School of Civil and Environmental Engineering, Cornell University
369 Hollister Hall, Ithaca, NY 14853
E-mail: pk285@cornell.edu

Abstract

The use of new materials and designs for which no significant experience exists as well as the aging structural infrastructure necessitates the development of methods that are able to continuously assess the structural integrity of the system. Even if during the design process its reliability has been accurately quantified, it is of paramount importance to update this prior knowledge and make informed predictions about its future reliability and operational capabilities. This is especially important as actual testing is either prohibitively expensive or practically impossible in simulating all the possible loading conditions.

Structural monitoring techniques should benefit from current capabilities in computational mechanics and make of use of sophisticated constitutive models (generally non-linear) of material/structural behavior. These have been shown to accurately capture the physics of deformation processes and have been incorporated in high fidelity computational tools (e.g. Finite Element Codes). Furthermore, recent advances in sensor technologies produce a large amount of data in real-time that should be analyzed in order to extract their informational content. Proposed techniques should provide robust estimates in the presence of significant uncertainties that arise from: a) unknown initial conditions, b) unknown loading conditions, c) model uncertainty, d) intermittent, noisy observations.

The present paper proposes a rigorous approach that provides quantitative measures and confidence intervals for: a) identification of state (i.e. response, material parameters, excitation) from incomplete observations, potentially in real-time. b) prognosis of system behavior/performance and updated estimates of its reliability, c) discerning the cost of current decisions in relation to the future health of the structure. For that purpose we employ a Bayesian framework coupled with Sequential Monte Carlo (SMC) sampling techniques.

1 Introduction

Despite the refinement in the mathematical models of material deformation and the prodigious increase in computational capabilities, our ability to predict the behavior of structural or mechanical systems has not necessarily improved due to the large number of uncertainties that appear in several model parameters. These uncertainties may be due to inherent variability of the physical system, approximations in the formulation of the problem, modeling errors in the solution of the approximate model, the lack of information about the system parameters.

The field of computational mechanics in particular has witnessed a revolution over the last few decades with the explosive developments in the field of Finite Elements and numerical methodologies in general (Blue Ribbon Panel on Simulation Based Engineering [4]). Today, we routinely utilize large finite element systems with hundreds of thousands or even million degrees of freedom to analyze the structural behavior of large systems such as ship hulls and platforms, aircrafts, under extreme loading and environmental conditions. Even though these models are accurate, their predictive ability requires information about material parameters, geometric dimensions and loading conditions

which are not always known. Even if extensive testing has been performed before the construction of the structural system, the actual implementation might exhibit deviations. Furthermore, several of these geometric or constitutive properties might change during the lifetime of the system due to damage accumulation, erosion from environmental effects etc.

It is of paramount importance therefore to develop efficient and robust system identification methodologies that are able to continuously monitor and quantitatively assess the structural integrity of the system. Furthermore they should update any prior knowledge and make informed predictions about its future reliability and operational capabilities. Such health monitoring techniques should benefit from the aforementioned capabilities in computational mechanics and Finite elements codes which are pervasive in the community.

Model-based system identification and particular damage detection in structural or mechanical systems has attracted considerable attention and several approaches have been proposed. These techniques can be broadly categorized distinguished as deterministic and probabilistic. The former attempt to solve an *inverse* problem by finding the system/model configuration that minimizes the mean square error between observations and model predictions. Hence the mathematical formulation reduces to an optimization problem for the solution of which several approaches such as neural networks, genetic algorithms, global search algorithms, have been employed. Probabilistic, Bayesian techniques on the other hand have gained prominence in recent years as they are able to deal in a principled manner with complex inference problems (Gelman et al. [1]). The basic premise of the Bayesian paradigm is the adoption of probability distributions for all unknown parameters that enter the model. Any information that is available to the analyst in advance, is encapsulated in the prior distribution. In fact the availability of a model for the system's response (e.g. Finite Element model) can be considered as a structured prior. Prior distributions are subsequently updated based on the evidence provided by the data through the likelihood function. The result of this process is the posterior distribution, which encompasses the effect of data in the prior hypotheses. Hence each possible configuration is associated with a measure of its plausibility which represents a combination of prior hypotheses and evidence provided by the data. An enticing aspect of the Bayesian formulation is the ability to incorporate physical knowledge and understanding in the otherwise abstract inference model, through the prior distribution. This readily establishes a bidirectional relationship between mechanics and statistics which is at the forefront of the project. Due to their probabilistic nature, Bayesian formulations can readily account for randomness or uncertainty in the collection of data or the model itself.

2 Proposed Methodology

We consider the most general case of a non-linear, multi-degree-of-freedom system characterized by a, generally, large system of coupled ordinary differential equations as follows:

$$\ddot{\mathbf{z}}_t + \mathbf{f}(\mathbf{z}_t, \dot{\mathbf{z}}_t, q_t) = \mathbf{e}_t \quad (1)$$

where \mathbf{z}_t is the vector displacements at time t , $\mathbf{f}(.)$ the nonlinear restoring force, \mathbf{e}_t the excitation, and q_t time-dependent model parameters, such as stiffness, mass or damping of structural members. This represents the general form of governing equations solved in standard Finite Element packages using various time integration schemes (e.g. Newmark, Runge-Kutta etc).

Even though a model is available for the evolution of the system, some or all of the parameters pertaining to the response (e.g. \mathbf{z}_t), excitation (\mathbf{e}_t) and model (q_t) are unknown. For economy of notation, let $\mathbf{x}_t = [\mathbf{z}_t, \dot{\mathbf{z}}_t, \mathbf{e}_t, q_t]^T$ denote the vector that completely specifies the unknown state of the structural system at any time t .

System identification must be performed based on the observations, denoted here by \mathbf{y}_t , which represents the data obtained by distributed sensors. These can be direct or indirect, partial or complete, measurements of the response quantities \mathbf{z}_t , $\dot{\mathbf{z}}_t$, $\ddot{\mathbf{z}}_t$ such as displacements, velocities, accelerations, loading \mathbf{e}_t (Equation (1)) such as acceleration, pressure, temperature time histories or model parameters q_t . It is important to point out is that these observations are generally *incomplete*, namely they do not provide sufficient information to identify uniquely the state of the system. For example, due to practical limitations, sensors cannot be positioned on every possible degree of freedom and therefore the observation vector \mathbf{y}_t is generally of much lower dimension than the response vector \mathbf{z}_t . Nevertheless the data obtained contain information about the whole system as response quantities are, to various extents, correlated. The task we address is rigorously assessing the information the data provides in order to infer the state of the system at that time instant. For economy of notation we denote by:

$$\mathbf{y}_t = \mathbf{g}(\mathbf{x}_t) + \mathbf{w}_t \quad (2)$$

the relation between observations (\mathbf{y}_t) and state parameters (\mathbf{x}_t) which is specified by a, generally, nonlinear deterministic filtering function, $\mathbf{g}()$. This is a mapping from “many-to-one”, that is several states \mathbf{x}_t give rise to the same \mathbf{y}_t . The term \mathbf{w}_t accounts for the observation error which can be due to the unavoidable noise that exists in any type of measurement or even systematic deviations due to sensor malfunctions for example. This essentially implies a *probabilistic* relation between observations and state and can be expressed by a probability density function $p(\mathbf{y}_t|\mathbf{x}_t)$ which represents the likelihood of observing \mathbf{y}_t given the state of the system \mathbf{x}_t at time t .

Based on the forward model Equation (1), we can define a probabilistic law for the evolution of the system’s state:

$$\dot{\mathbf{x}}_t = \mathbf{h}(\mathbf{x}_t, \mathbf{v}_t) \quad (3)$$

where where $\mathbf{h}()$ is a deterministic nonlinear function:

$$\mathbf{h}(\mathbf{x}_t, \mathbf{v}_t) = \begin{bmatrix} \dot{z}_t \\ (\mathbf{e}_t - f(z_t, \dot{z}_t, \mathbf{q}_t)) + v_{t,m} \\ v_{t,e} \\ v_{t,q} \end{bmatrix} \quad (4)$$

and $\mathbf{v}_t = [v_{t,m}, v_{t,e}, v_{t,q}]^T$ are noise terms (which can be thought of as normally distributed) that indicate uncertainty in the forward model, excitation and model parameters respectively.

In summary, we have described a general, probabilistic model that relates the unknown state of the naval system and its evolution with the stream of sensor data. This model accounts for uncertainties in the discretized Finite Element model, the evolution of model parameters and loading sequence and is characterized by three sets of probability distribution functions: a) Transition density $p_r(\mathbf{x}_t | \mathbf{x}_{t-1})$ which expresses the probability of being at state \mathbf{x}_t at time t if the system was at state \mathbf{x}_{t-1} at the previous time step $t-1$, b) Emission density $p_e(\mathbf{y}_t | \mathbf{x}_t)$ which expresses the probability of observing \mathbf{y}_t if the system is at state \mathbf{x}_t at time t , and c) Initial conditions density $p(\mathbf{x}_0)$ which represents uncertainty about the initial state of the system. This distribution can be very diffuse or even uniform in the absence of any prior information.

System identification then reduces to determining the probability distribution for the states $\mathbf{x}_{0:t} = (\mathbf{x}_0, \mathbf{x}_1, \mathbf{x}_2, \dots, \mathbf{x}_t)$ given the observations $\mathbf{y}_{1:t} = (\mathbf{y}_1, \mathbf{y}_2, \dots, \mathbf{y}_t)$, i.e. $p(\mathbf{x}_{0:t} | \mathbf{y}_{1:t})$. Using Bayes’ rule this can be written as:

$$p(\mathbf{x}_{0:t} | \mathbf{y}_{1:t}) = \frac{p(\mathbf{y}_{1:t} | \mathbf{x}_{0:t})p(\mathbf{x}_{0:t})}{Z(\mathbf{y}_{1:t})} \quad (5)$$

where $Z(\mathbf{y}_{1:t}) = \int p(\mathbf{y}_{1:t} | \mathbf{x}_{0:t})p(\mathbf{x}_{0:t})d\mathbf{x}_{0:t}$ is the normalizing constant that is independent of the system’s state. One observes that:

- $p(\mathbf{x}_{0:t})$ plays the role of the prior distribution on the states $\mathbf{x}_{0:t}$ and encapsulates the information/knowledge we have about the system before looking at the observations. This is represented by the model prescribed in Equation (1) and the evolution laws of Equation (4)). Therefore, the emission density can be readily expressed as:

$$p(\mathbf{x}_{0:t}) = p(\mathbf{x}_0) \prod_{j=1}^t p_r(\mathbf{x}_j | \mathbf{x}_{j-1}) \quad (6)$$

where $p_0(\mathbf{x}_0)$ is the (prior) distribution on the initial state of the system which is generally uncertain.

- $p(\mathbf{y}_{1:t} | \mathbf{x}_{0:t})$ plays the role of the likelihood function which quantifies the plausibility of observing $\mathbf{y}_{1:t}$ for any possible state $\mathbf{x}_{0:t}$. It can be expressed as: $p(\mathbf{y}_{1:t} | \mathbf{x}_{1:t}) = \prod_{j=1}^t p_e(\mathbf{y}_j | \mathbf{x}_j)$

Determining $p(\mathbf{x}_{0:t} | \mathbf{y}_{1:t})$ is analytically intractable due to nonlinearities in the evolution and emission laws (Equations (2), (3)). Previous attempts using signal processing tools such as the Kalman Filter (Kalman [2]) and variations thereof (i.e. extended Kalman filter, unscented Kalman Filter) can at best provide approximate solutions and might require linearization of the governing equations. In contrast, we propose a *non-intrusive* Monte Carlo inference framework that can readily utilize deterministic Finite Element models as black boxes *without* any alterations. Hence models that are well-established and might have already been constructed during the design phase can be used in order to identify the state of the system and predict its future operational capabilities.

Inference of the posterior density $p(\mathbf{x}_{0:t} \mid \mathbf{y}_{1:t})$ (Equation (5)) is analytically intractable, except for some special cases as for linear systems and Gaussian noise. We propose employing Sequential Monte Carlo (SMC) methods. They represent a set of flexible simulation-based methods for sampling from a sequence of probability distributions (Liu [3]). As with Markov Chain Monte Carlo methods (MCMC) which are most commonly used for Bayesian inference, the target distribution(s) need only be known up to constant and therefore do not require calculation of the intractable integral for $Z(\mathbf{y}_{1:t})$ in Equation (5).

SMC methods operate on a sequence of probability distributions as those defined in Equation (5) by considering various time instants, t . They utilize a large set of random samples, named particles, which are propagated over time using simple importance sampling, resampling and rejuvenation mechanisms. Each of these particles, which can be thought of as a possible configuration of the system's state, is associated with a weight the value of which is proportional to the likelihood of the respective configuration based on the available data. These weights are updated sequentially, that is every time a new datum y_t arrives and therefore require the solution of the governing ODEs (Equations (1) or (3)) for a *single time step*. This is simply done by a call to the Finite Element solver which is appropriately initialized. Hence the cost of running computationally expensive forward solvers (i.e. Finite Element codes) is minimized by performing runs in concentrated but informative regions of the state space. The samplers proposed are directly parallelizable as the evolution of each particle is by-and-large independent of the rest. Hence given a sufficient number of processors one can envision performing the identification and updating of the system's state in *real time*.

An advantage of the model-based framework advocated in this proposal, is that the inference results can be readily used to make predictions about the system's behavior under future excitations. Predictive estimates can be readily computed and updated at any phase of the inference process. At any time instant t , these predictions are based on the posterior distribution $p(\mathbf{x}_{0:t} \mid \mathbf{y}_{1:t})$ and therefore encapsulate the information provided by the observations made up to this point. Consider the case that predictions involving the state of the system \mathbf{x}_T at a future time $T > t$ are of interest. In order to account for the uncertainty about the current and future evolution, we are interested in calculating the probability distribution $p(\mathbf{x}_T \mid \mathbf{y}_{1:t})$. This expresses the relative likelihood of various future states \mathbf{x}_T given all the data $\mathbf{y}_{1:t}$ available up to present. Based on the equations above this can readily be estimated as follows:

$$\begin{aligned} p(\mathbf{x}_T \mid \mathbf{y}_{1:T}) &= \int p(\mathbf{x}_T, \mathbf{x}_{0:t}, \mathbf{x}_{t+1:T-1} \mid \mathbf{y}_{1:t}) d\mathbf{x}_{0:t} d\mathbf{x}_{t+1:T-1} \\ &= \int \left(\prod_{j=t+1}^T p_\tau(\mathbf{x}_j \mid \mathbf{x}_{j-1}) \right) p(\mathbf{x}_{0:t} \mid \mathbf{y}_{1:t}) d\mathbf{x}_{0:t} d\mathbf{x}_{t+1:T-1} \end{aligned} \quad (7)$$

The second term in the integrand, $p(\mathbf{x}_{0:t} \mid \mathbf{y}_{1:t})$ is the posterior distribution approximated in the SMC scheme presented earlier by a number of particles and associated weights $\{\mathbf{X}_{0:t}^{(i)}, W_t^{(i)}\}$. The remaining terms in the integrand correspond to the prior distribution for the evolution of the system as defined previously (e.g. Equation (6)). As this high dimensional integration is analytically intractable we can use Monte Carlo estimates based on samples drawn from the distributions in the integrand.

References

- [1] A Gelman, JB Carlin, HS Stern, and DB Rubin. *Bayesian Data Analysis*. Texts in Statistical Science. 2nd edition, 2003.
- [2] RE Kalman. A new approach to linear filtering and prediction problems. *Transactions of the ASME - Journal of Basic Engineering*, 82:35–45, 1960.
- [3] J.S. Liu. *Monte Carlo Strategies in Scientific Computing*. Springer Series in Statistics. Springer, 2001.
- [4] Blue Ribbon Panel on Simulation Based Engineering. Revolutionizing engineering science through simulation. Technical report, National Science Foundation, 2006.

Prediction of maximum deflection of double layer grid space structure using neural networks

Reza KAMYAB MOGHADAS*, Kok Keong CHOONG, Sabarudin MOHD

* M.Sc. of Civil Engineering
Iranian Academic Center for Education, Culture, and Research, Kerman, Iran
r_kamyab_m@yahoo.com

Abstract

Efficient neural networks models are trained to predict the maximum deflection of two-way on two-way grids with variable geometrical parameters (span and height) as well as cross-sectional areas of the element groups. Backpropagation (BP) and radial basis function (RBF) neural networks are employed for the mentioned purpose. The inputs of the neural networks are the length of the spans, L , the height, h , and cross-sectional areas of all groups, A , and the outputs are maximum deflections of the corresponding double layer grids, respectively. The numerical results indicate that the RBF neural network is better than BP in terms of training time and performance generality.

1. Introduction

Many thousands of impressive space structures have been built all over the world for covering sport stadiums, gymnasiums, leisure centers, aircraft hangars, railway stations and many other purposes. A number of these structures have spans of well over 200m. Due to their three dimensional action, space structures are very efficient structural systems to carry heavy loads as well as to span large distances. As the use of space structures becomes more popular, it is essential to evolve strategies for their convenient analysis and design. In the present investigation, neural network techniques are employed for this purpose. Over the last decade, artificial intelligence techniques have emerged as a robust tool to replace time consuming procedures in many scientific or engineering applications. The use of neural networks to predict finite element analysis outputs has been studied previously in the context of many engineering applications [1-3]. The principal advantage of a properly trained neural network is that it requires a trivial computational effort to produce an approximate solution.

The main aim of the present work is to train neural networks for predicting the maximum deflection of double layer grid space structures for static loadings. Backpropagation (BP) and radial basis function (RBF) neural networks are employed.

2. Backpropagation Neural Network

The most popular and successful learning method for training the multilayer neural networks is the backpropagation algorithm. The development of the Backpropagation learning was reported by Rumelhart Hinton and Williams [4]. The algorithm employs an iterative gradient-descent method of minimization which minimizes the mean squared error between the desired output and network output. The backpropagation training procedure is presented below.

Let

$$E = \frac{1}{2} \sum_{j=1}^N \sum_{i=1}^M e_i^2(n) \quad (1)$$

N , M , and n are number of training input patterns, dimension of output space, and number of iterations, respectively.

$$e_i(n) = d_i(n) - y_i^{(L)}(n) \quad (2)$$

where L represent the output layer.

$$v_i^l(n) = \sum_{j=1}^N w_{ij}^{(l)} y_j^{(l-1)}(n) \quad (3)$$

where $y_j^{(l-1)}(n)$ is the function signal of neuron j in the previous layer ($l-1$) at iteration n . $w_{ij}^{(l)}(n)$ is the weight of neuron i in layer l that is fed from neuron j in layer $(l-1)$. Then the output signal of neuron i in layer l is

$$y_i^l(n) = f(v_i^l(n)) \quad (4)$$

where $f(\cdot)$ is the activation function. If neuron i is in the first hidden layer ($l=1$), then set $y_i^0(n) = x_i(n)$. Backward computation (local gradients)

$$\ddot{a}_i(n) = -\frac{\partial E_i}{\partial v_i} \quad (5)$$

is called the local error or local gradients. Equation (5) can be simplified to

for neuron i in output layer L :

$$\ddot{a}_i^L(n) = e_i^L(n) f'(v_i^L(n)) \quad (6)$$

for neuron i in hidden layer l :

$$\ddot{a}_i^l(n) = f'(v_i^l(n)) \sum_k \ddot{a}_k^{(l+1)}(n) w_{ki}^{(l+1)}(n) \quad (7)$$

where $f'(\cdot)$ is the derivative of the activation function with respect to $v(n)$. If the activation function is chosen to be the hyperbolic tangent function, then $f'(\cdot)$ is:

$$f'(v_i) = \frac{d f(v_i)}{d v_i} = \tilde{\alpha}(1 - f^2(v_i)) \quad (8)$$

Hence, adjust the weights of the network in layer l according to the generalized delta rule:

$$w_{ij}^{(l)}(n+1) = w_{ij}^{(l)}(n) + \mu \ddot{a}_i^{(l)}(n) y_j^{(l-1)}(n) \quad (9)$$

where μ is the positive constant learning rate, usually equals to 0.01. If after updating the weights, the error E is not minimized, new iterations are required.

3. Radial Basis Function Neural Network

The backpropagation algorithm for the design of a multilayer neural network described earlier may be viewed as a form of stochastic approximation. Radial basis functions (RBFs) take a different approach by viewing the design of a neural network as a curve-fitting problem by finding a best fit to the training data in a multidimensional space. The use of RBF in the design of neural networks was first introduced by Broomhead and Lowe [5]. The RBF network basically involves three entirely different layers; an input layer, a hidden layer of high enough dimension, and an output layer. The transformation from the hidden unit to the output space is linear. Each output node is the weighted sums of the outputs of the hidden layer. However, the transformation from the input layer to the hidden layer is nonlinear. Each neuron or node in the hidden layer forming a linear combination of the basis (or kernel) functions which produces a localized response with respect to the input signals. This is to say that RBF produce a significant nonzero response only when the input falls within a small localized region of the input space. The most common basis of the RBF is a Gaussian function of the form:

$$\varphi_l(\vec{x}) = \exp\left[-\frac{(\vec{x} - \vec{c}_l)^T (\vec{x} - \vec{c}_l)}{2\delta_l}\right], \quad l = 1, 2, \dots, P \quad (10)$$

where φ_l is the output of the l th node in hidden layer, \vec{x} is the input pattern, \vec{c}_l is the weight vector for the l th node in hidden layer, i.e., the center of the Gaussian for node l ; δ_l is the normalization parameter (the measure of spread) for the l th node, and P is the number of nodes in the hidden layer. The outputs are in the range from zero to one so that the closer the input is to the center of the Gaussian, the larger the response of the node. The name RBF comes from the fact that these Gaussian kernels are radially symmetric; that is, each node produces an identical output for inputs that lie a fixed radial distance from the center of the kernel \vec{c}_l . The network outputs are given by:

$$y_i = \vec{w}_i^T \varphi_l(\vec{x}) \quad , \quad i = 1, 2, \dots, Q \quad (11)$$

where y_i is the output of the i th node, \vec{w}_i is the weight vector for this node, Q is the number of nodes in the output layer, and $\varphi_l(\vec{x})$ is the vector of outputs from the hidden layer (augmented with an additional component or a bias which assumes a value of one).

No actual training for the hidden layer of RBF networks is required. Instead, the transpose of training input matrix is taken as the layer weight matrix. In order to design neural networks, MATLAB is employed. In order to produce the training set, a computer program is developed. The structural analysis is based on the finite element formulation of the displacement method.

4. Results and Discussion

The double layer grid considered is the type of two-way on two-way and the bar elements are connected by MERO type of joints. Each span contains 15 bays of equal length in both directions. The structure is assumed to be supported at corners of bottom layer each on three nodes. The double layer grid is shown in Fig. 1. The span, L , is varied between 25 and 75 m with steps of 5 m. The height, h , is varied between $0.035L$ and $0.095L$ with steps of 0.2 m. Due to practical demands, members are grouped. Cross-sectional areas of the groups, A , are selected from a list of available tube sections in STAHL as: 175, 195, 222, 275, 307, 379, 402, 451, 588, and 719 cm^2 , respectively. In this work, three element groups are considered ; that is, all the top, bottom and web layer elements are grouped in groups 1 to 3, respectively. The sum of dead and live loads of 250 kg/m^2 is applied to the nodes of the top layer.

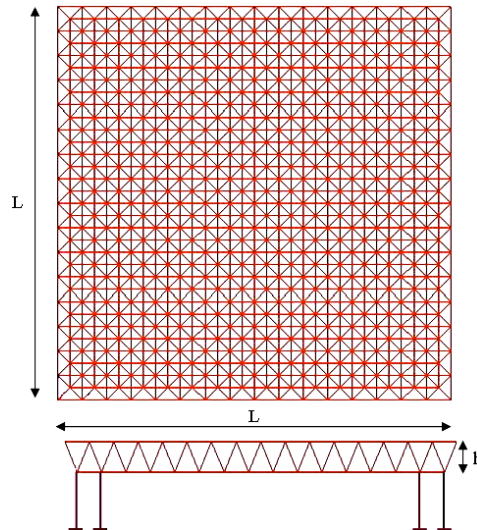


Fig. 1. Double layer grids (two-way on two-way)

Data Selection and Neural Networks Training

Inputs of the neural networks are the length of the span, L , the height, h , and cross-sectional areas of all the groups, $A_1; A_2; A_3$, while the outputs are maximum deflections of the corresponding double layer grids. Backpropagation (BP) and radial basis function (RBF) neural networks are employed. In order to provide the training set a computer program is developed. In this program, the randomly produced double layer grids are analyzed and their maximum deflections are saved as the output vectors components. The structural analysis is based on the finite element formulation of the displacement method. As the size of problem is very large, a training set including 3500 samples is produced. From which, 3000 and 500 samples are selected to train and test the performance generality of the neural networks, respectively. The results of generality testing of the BP and RBF networks are summarized in Table 2. Error percentages of the neural networks in testing phase are also shown in Figs. 3 to 4.

<i>Network</i>	<i>Training time (sec.)</i>	<i>Max. Error (%)</i>	<i>Mean. Error (%)</i>
BP	492.50	34.693	4.982
RBF	47.72	14.304	2.554

Table 2. Errors of BP and RBF networks

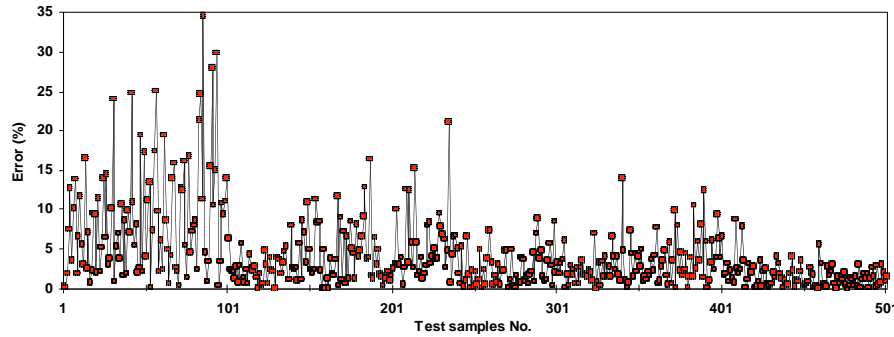


Fig. 3. Errors of BP network in test phase

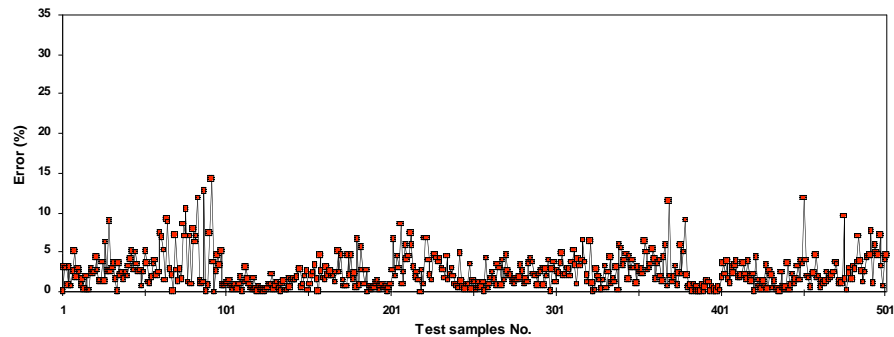


Fig. 4. Errors of RBF network in test phase

5. Conclusion

Backpropagation (BP) and radial basis function (RBF) neural networks have been employed to predict the maximum deflection of two-way on two-way grids. Numerical results have shown that the RBF is better than BP neural network in terms of training time and performance generality.

References

- [1] Hajela P, Berke L. Neurobiological computational models in structural analysis and design. *Computers & Structures* 1991; **41**:657–667.
- [2] Berke L, Patnaik SN, Murthy PLN. Optimum design of aerospace structural components using neural networks. *Computers & Structures* 1993; **48**:1001–1010.
- [3] Theocaris PS, Panagiotopoulos PD. Neural networks for computing in fracture mechanics: methods and prospects of applications. *Computer Methods in Applied Mechanics and Engineering* 1993; **106**:213–228.
- [4] Haykin S. *Neural Networks: A Comprehensive Foundation*, Macmillan, New York, NY, 1994.
- [5] Wasserman PD. *Advanced Methods in Neural Computing*, New York: Prentice Hall Company, Van Nostrand Reinhold; 1993.